

ECONOMIC GEOLOGY RESEARCH INSTITUTE HUGH ALLSOPP LABORATORY

University of the Witwatersrand
Johannesburg

**AMPHIBOLITE FACIES METAMORPHISM OF FIG
TREE GROUP METASEDIMENTS: A RECORD OF THE
MID-CRUSTAL RESPONSE TO ~3.23GA TERRANE
ACCRETION IN THE BARBERTON GREENSTONE
BELT, SOUTH AFRICA**

**G. STEVENS, G.T.R. DROOP, R.A. ARMSTRONG
AND C.R. ANHAEUSSER**

UNIVERSITY OF THE WITWATERSRAND
JOHANNESBURG

**AMPHIBOLITE FACIES METAMORPHISM OF FIG TREE GROUP
METASEDIMENTS: A RECORD OF THE MID-CRUSTAL RESPONSE TO
~3.23GA TERRANE ACCRETION IN THE BARBERTON GREENSTONE BELT,
SOUTH AFRICA**

by

G. STEVENS¹, G.T.R. DROOP², R.A. ARMSTRONG³ AND C.R. ANHAEUSSER⁴

*(¹Department of Geology, University of Stellenbosch, 7602 Matieland, South Africa;
²Department of Earth Sciences, University of Manchester, Oxford Road, Manchester
M139PL, UK; ³Research School of Earth Sciences, The Australian National University,
Canberra, 0200 ACT, Australia; ⁴Economic Geology Research Institute-Hugh Allsopp
Laboratory, University of the Witwatersrand, Private Bag 3, P.O. WITS 2050, South Africa)*

**ECONOMIC GEOLOGY RESEARCH INSTITUTE
INFORMATION CIRCULAR No. 354**

October, 2001

**AMPHIBOLITE FACIES METAMORPHISM OF FIG TREE GROUP
METASEDIMENTS: A RECORD OF THE MID-CRUSTAL RESPONSE TO
~ 3.23 GA TERRANE ACCRETION IN THE BARBERTON GREENSTONE BELT,
SOUTH AFRICA**

ABSTRACT

The Schapenburg schist belt is one of several large greenstone remnants exposed in the granitoid-dominated terrane to the south of the Barberton greenstone belt. Schapenburg is unique amongst the many greenstone remnants in this area in that it contains a well-developed metasedimentary sequence in addition to the typical mafic-ultramafic volcanic rocks. Detrital zircons within the metasediments have ages as young as 3.23 Ga. Thus, these metasediments correlate with Fig Tree Group rocks exposed in the central portions of the Barberton greenstone belt some 60 km to the north, where they are metamorphosed to greenschist facies conditions. The Schapenburg metasediments are relatively K₂O-poor, and are commonly characterised by the peak metamorphic assemblage garnet + cordierite + gedrite + biotite + quartz \pm plagioclase. Other assemblages recorded are garnet + cummingtonite + biotite + quartz, cordierite + biotite + sillimanite + quartz and cordierite + biotite + anthophyllite. In all cases the peak assemblages are texturally very well equilibrated and the predominantly almandine garnets from all rock types show almost flat zonation patterns for Fe, Mg, Mn and Ca. Analysis using KCFMASH reaction relations, as well as a variety of geothermometers and barometers, has constrained the peak metamorphic pressure-temperature conditions to 640 \pm 40 °C and 4.8 \pm 1.0 kbar. The strong bedding-parallel foliation in the metasediments dips to the east at an angle of 75 to 85°. In this foliation plane elongated cordierite rods, produced during prograde metamorphism, define a close to vertical mineral lineation. Post-kinematic and peak metamorphic anthophyllite and garnet overgrow this fabric. The sedimentary sequence youngs to the east, and in this direction is overlain by a layered volcanic sequence of komatiites and komatiitic basalts of the Onverwacht Group, which young in the same direction. Collectively, these observations are consistent with metamorphism driven by crustal thickening that was accomplished by thrusting to the northwest at approximately 3.23 Ga and burial of the sediments to mid-crustal depths. Peak conditions were attained after deformation, probably as a result of the re-establishment of isotherms disrupted during crustal thickening.

_____oOo_____

**AMPHIBOLITE FACIES METAMORPHISM OF FIG TREE GROUP
METASEDIMENTS: A RECORD OF THE MID-CRUSTAL RESPONSE TO
~ 3.23 GA TERRANE ACCRETION IN THE BARBERTON GREENSTONE BELT,
SOUTH AFRICA**

CONTENTS

	Page
INTRODUCTION	1
TECTONIC HISTORY OF THE BARBERTON GREENSTONE BELT	3
PREVIOUS METAMORPHIC STUDIES	4
GEOLOGY OF THE STUDY AREA	5
GEOCHRONOLOGY	8
METAMORPHISM OF THE METATURBIDITE SEQUENCE	8
MINERAL CHEMISTRY	9
PEAK METAMORPHIC CONDITIONS	9
DISCUSSION	13
ACKNOWLEDGEMENTS	14
REFERENCES	14

_____oOo_____

**Published by the Economic Geology Research Institute
(incorporating the Hugh Allsopp Laboratory)
School of Geosciences
University of the Witwatersrand
1 Jan Smuts Avenue
Johannesburg 2001
South Africa**

<http://www.wits.ac.za/egru/research.htm>

ISBN 1-86838-289-3

**AMPHIBOLITE FACIES METAMORPHISM OF FIG TREE GROUP
METASEDIMENTS: A RECORD OF THE MID-CRUSTAL RESPONSE TO
~3.23 GA TERRANE ACCRETION IN THE BARBERTON GREENSTONE BELT,
SOUTH AFRICA**

INTRODUCTION

The Schapenburg schist belt forms part of the geology of the Barberton Mountain Land. This term encompasses two main geological components, namely the Barberton greenstone belt, and the collection of gneissic and undeformed granitoids that surround the greenstone belt (Fig. 1). The Barberton greenstone belt consists of probably the best preserved, early Archaean (3.5-3.2 Ga) volcano-sedimentary succession on earth (Fig. 1). The sequence exposed in the belt has been assigned to the Barberton Supergroup (Ward, 1999) and comprises of three major lithostratigraphic units. From the base upward, these are:

(1) the 3.50 to 3.30 Ga Onverwacht Group, composed largely of mafic and ultramafic volcanic rocks, with minor units of felsic volcanic and volcanoclastic rocks, as well as sediments;

(2) the 3.26 to 3.22 Ga predominantly argillaceous Fig Tree Group comprising a succession of greywackes, cherts, shales, and including some dacitic flows and fragmental volcanic rocks; and

(3) the ~3.2 Ga Moodies Group, which consists of an arenaceous sedimentary unit composed largely of feldspathic and quartzitic sandstones, polymictic conglomerates, lesser amount of siltstone and shale, and thin units of basalt, jaspilite, and magnetite-bearing shale.

The granitoid rocks surrounding the greenstone belt vary in composition from tonalite through trondhjemite, granodiorite and granite to syenite (Anhaeusser and Robb, 1980; Robb and Anhaeusser, 1983). Previously the granitoids were regarded as having evolved through 3 magmatic cycles, with systematic variation from tonalites and trondhjemites in the oldest cycle, to granites in the youngest cycle (e.g., Anhaeusser and Robb, 1981). Recent dating using U/Pb zircon techniques has revealed a spread of emplacement ages for each granitoid type, rather than ordered cycles (Armstrong et al., 1990; Kamo and Davis, 1994; Kröner et al., 1991a, 1996).

According to a recent compilation by de Ronde and Kamo (2000) the oldest granitoid rocks are exposed along the southern margin of the belt where the trondhjemitic Steynsdorp pluton (3490 ± 4 Ma), in the southeast corner of the belt, represents the oldest intrusive granitoid rock in the Barberton Mountain Land. Northwest of the Steynsdorp pluton, the trondhjemitic Stolzburg (3445 ± 3 Ma), Doornhoek (3448 ± 8 Ma) and Theespruit (3443 ± 3 Ma) plutons probably represent the consequence of a single magmatic episode at approximately 3.45 Ga. A younger generation of magmatism at about 3.22 Ga is represented by the tonalitic Kaap Valley pluton (3227 ± 1 Ma), the trondhjemitic Nelshoogte pluton (3236 ± 1 Ma) and the granodioritic Dalmein pluton ($3216 \pm 2/-1$ Ma). The felsic magmatic history of the Barberton Mountain Land terminated at approximately 3.11 Ga with the intrusion of the Nelspruit, Heerenveen and Mpuluzi (c. 3107 Ma) batholiths, as well as the Boesmanskop syenite (3107 ± 2 Ma) (Anhaeusser et al., 1983; Anhaeusser and Robb, 1983; de Ronde and Kamo, 2000; Kamo and Davis, 1994; Robb et al., 1983).

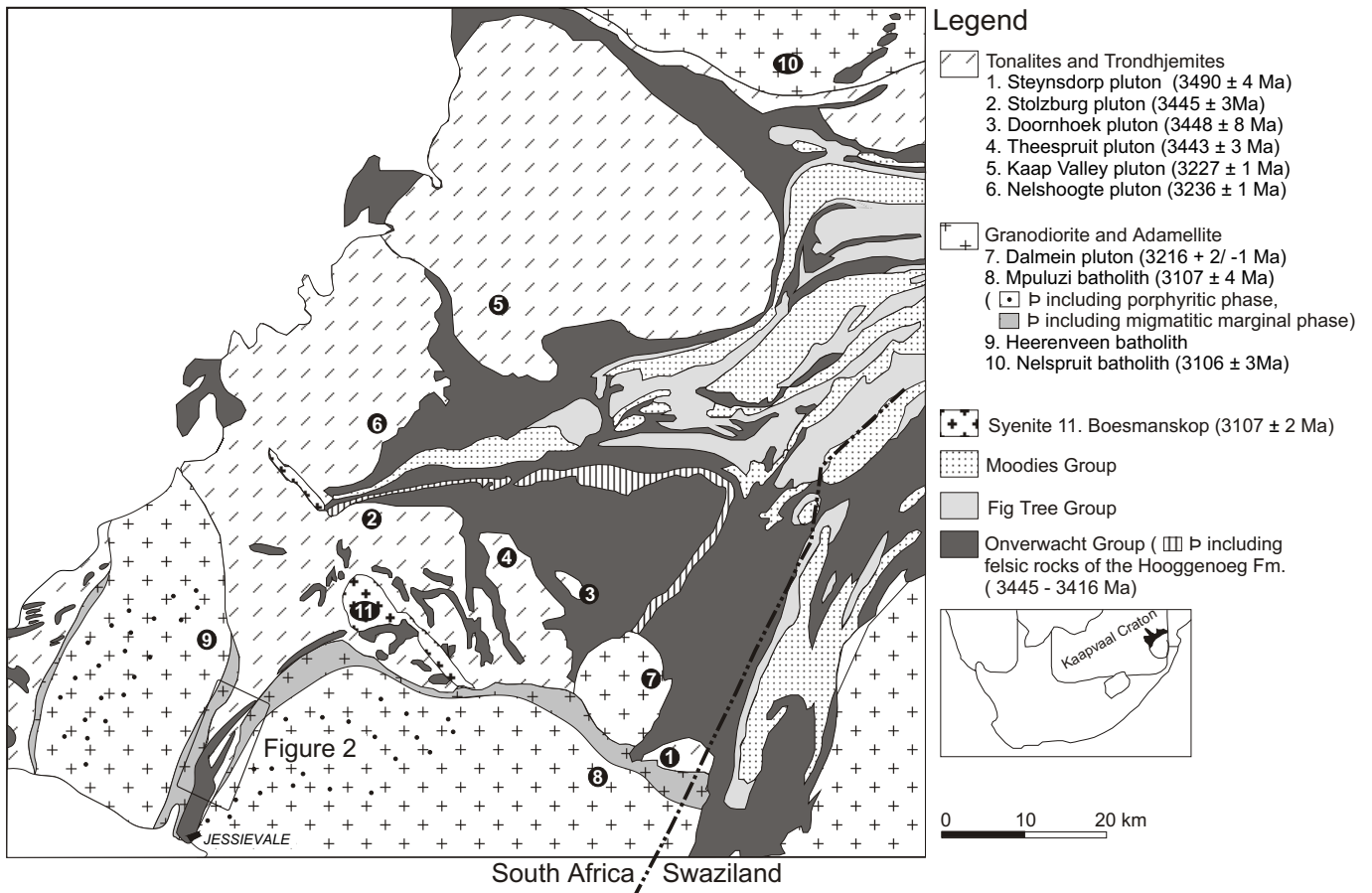


Figure 1: The southern portion of the Barberton greenstone belt and surrounding granitoid terrane modified after de Ronde and de Wit (1994). The geochronological data on the granitoid rocks are from de Ronde and Kamo (2000).

Since the 1960s the Barberton greenstone belt has been recognized as an important Archaean terrane that records processes relating to early crustal development and cratonization. Recently, advances have been made in understanding the tectonic and magmatic evolution of the rocks of the Barberton Mountain Land. Particularly, there is now good evidence for at least two major compressive tectonic events associated with the voluminous calc-alkaline magmatism at *c.* 3.45 Ga and 3.22 Ga. In the modern rock record such events at actively convergent plate margins have well documented and characteristic metamorphic signatures, yet in the Barberton greenstone belt no clear understanding exists regarding the pattern of metamorphism associated with either of these events, despite the obvious importance of such information to the understanding of crustal processes during Archaean times. In the Theespruit pluton sphene ages are some 200 Ma younger than the magmatic age established from zircon geochronology (Kamo and Davis, 1994) and potentially correlate with the 3.22 Ga tectono-magmatic event. Thus, the many greenstone xenoliths occurring in the granitoid gneiss terrane to the south of the greenstone belt may offer the best possibility for studying the metamorphic signature of this event as the trondhjemitites are not compositionally suited to providing a detailed metamorphic record. This study therefore examines the metamorphic history of the Schapenburg schist belt, one of the larger greenstone remnants from this area, in an effort to begin to constrain the metamorphic response to tectonism in the Barberton Mountain Land.

TECTONIC HISTORY OF THE BARBERTON GREENSTONE BELT

Early views of the greenstone belt saw the entire approximately 25km-thick stratigraphy as constituting a continuous volcanosedimentary succession (Viljoen and Viljoen, 1969; Anhaeusser, 1978). The largely vertical orientation of the stratigraphy was seen as a consequence of deformation during diapiric intrusion of the tonalite and trondhjemitic bodies that are exposed in contact with the Onverwacht Group rocks from many areas surrounding the belt. Subsequent research has identified processes more readily reconcilable with models of lateral plate motion, and has linked these tectonic events to the well-defined magmatic episodes identified in the related granitoid rocks. Consequently, a complex, polyphase and protracted tectono-magmatic history has begun to emerge (e.g., de Wit, 1982; Armstrong et al., 1990; de Ronde and de Wit, 1994; Kamo and Davis, 1994; Lowe, 1999; de Ronde and Kamo, 2000).

High precision single zircon geochronology (e.g., Kamo and Davis, 1994; de Ronde and Kamo, 2000) has confirmed earlier suggestions that the stratigraphy of the greenstone belt includes major structural breaks and tectonic repetitions (e.g., de Wit, 1982, 1991). The oldest rocks dated so far are felsic schists exposed in the Steynsdorp anticline (3544 ± 3 to 3547 ± 3 Ma, Kröner et al., 1996). In this region, the Steynsdorp pluton and the rocks of the Steynsdorp anticline record evidence for a deformation episode that predates the deposition of the bulk of the Onverwacht Group (Kisters and Anhaeusser, 1995). Thus, the Steynsdorp anticline has been interpreted to represent the oldest nucleus of the belt, onto which the overlying rocks of the Onverwacht Group were tectonically and magmatically accreted (e.g., Kröner et al., 1996; Lowe, 1994, 1999).

The next recorded tectono-magmatic episode involved the formation of recumbent nappes and downward-facing sequences in response to horizontal shortening of the Onverwacht Group in the southern part of the belt (e.g., de Wit, 1982; de Wit et al., 1987). During this period the rocks above the Komati fault were amalgamated with the underlying Theespruit Formation (e.g., de Wit, 1991; de Ronde and de Wit, 1994). Deformation was associated with intense calc-alkaline magmatic activity that produced the *c.* 3.45 Ga trondhjemitic plutonism at the southern margin of the belt, as well as the formation of extrusive felsic equivalents in the Theespruit and Hooggenoeg Formations (e.g., de Wit et al., 1987; de Ronde and de Wit, 1994). U-Pb and Pb-Pb zircon ages on syntectonic felsic intrusions indicate that this deformational episode occurred between 3445 and 3416 Ma (e.g., Kröner and Todt, 1988; Armstrong et al., 1990; Kamo and Davis, 1994).

Tectonic wedges of *c.* 3538 Ma tonalite gneisses preserved in the *c.* 3453 Ma old Theespruit Formation, as well as the presence of ancient xenocrystic zircons in the Steynsdorp pluton have been used to confirm the presence of an older sialic basement prior to this event (Armstrong et al., 1990). Most of the deformation recorded in the present exposures of the belt is believed to have occurred during a short-lived compressional tectonic event, which coincided with the syndeformational deposition of the Upper Fig Tree and Moodies Group sediments and the *c.* 3.22 Ga calc-alkaline magmatism (e.g., Kamo and Davis, 1994). This event was probably responsible for the upright, tight to isoclinal folding, the formation of thrust faults, and the amalgamation of the northern and southern parts of the greenstone belt along a major suture zone in the centre of the belt (the Saddleback-Inyoka fault system - de Ronde and de Wit, 1994). Age estimates on pre- and post-tectonic intrusions in the northern part of the belt indicate that this deformation event occurred over a period of 3 million years (between 3229-3226 Ma - Kamo and Davis, 1994; de Ronde and Kamo, 2000).

The emplacement of large volumes of sheet-like potassic granites, during the *c.* 3.1 Ga magmatic event marked the final stabilization of the greenstone belt and its surroundings. It has been suggested that this late-tectonic history of the belt was associated with a change from convergent to transtensional (extensional) tectonics (de Ronde and de Wit, 1994).

PREVIOUS METAMORPHIC STUDIES

Despite substantial advances in understanding the tectono-magmatic framework, the relationship of metamorphism to tectonic and magmatic processes in the belt remains vague. In general terms, the belt is characterized by lower- to mid-greenschist facies assemblages in the central portions and higher-grade amphibolites from the margins and from greenstone xenoliths in the surrounding granitoids. In the central portions of the belt Xie et al. (1997), using an empirical calibration of the chlorite-geothermometer, estimated a temperature of $\sim 320^{\circ}\text{C}$ for the pervasive greenschist facies metamorphism. In the south-central parts of the belt this metamorphism has been interpreted to be a result of both seafloor and subsequent burial metamorphism during Onverwacht Group deposition (Cloete, 1991).

Cloete (1991, 1999) using mineral composition isopleth maps (chlorite, amphibole, plagioclase), the plagioclase-amphibole geothermometer, and fluid inclusions from quartz-filled interpillow cavities, estimated the P-T conditions for the 3490 Ma Komati Formation, to be approximately 4 kbar and 520°C . Retrogression occurred at 2.5 kbar and approximately 350°C . The peak metamorphic assemblage has been related to an early anticlockwise path produced in an extensional regime (i.e., burial metamorphism during the formation of the volcanic sequence). Several studies propose that this peak metamorphic event was synchronous with the deposition of the upper Onverwacht Group, and predated the intrusion of the Theespruit pluton (e.g., De Wit et al., 1982; López Martínez et al., 1984; Armstrong et al., 1990). Cloete (1999) interpreted the retrogression as occurring in response to later clockwise path caused by compressional tectonics during the intrusion of the Theespruit pluton at ~ 3440 Ma.

The amphibolite facies assemblages from the margins of the belt, where the greenstone sequence is commonly in contact with tonalite or trondhjemite plutons, and in greenstone xenoliths in these plutonic rocks (Fig. 1), has been regarded as a subsequent contact-metamorphic overprint associated with magma emplacement (e.g., Anhaeusser, 1969; Cloete, 1991; Harris et al., 1993). Anhaeusser and Viljoen (1965) proposed that these amphibolite facies marginal zones grade into lower- or sub-greenschist grade rocks over distances of 5 to 8 km.

To date the only detailed study focusing on the greenstone remnants south of the Barberton greenstone belt has been based on xenoliths east of the Boesmanskop syenite. Here, peak metamorphic assemblages consisting of (1) diopside + andesine + garnet + quartz in calcic and magnesian clastic sediments; (2) magnesio-hornblende + andesine + quartz in metamafic volcanic rocks; and (3) quartz + ferrosilite + magnetite + grunerite in iron formation layers, have been documented by Dziggel et al. (2001). Retrogression is marked by epidote replacing the peak metamorphic assemblage in the clastic sediments, actinolitic rims around peak metamorphic magnesio-hornblende cores in the metamafic rocks, and by a second generation of grunerite that occurs as fibrous aggregates rimming orthopyroxene in the iron formations. P-T calculations for the peak-metamorphic mineral assemblages in

all these rock types vary between 650-700°C and 8-10 kbar. Dziggel et al. (2001) have interpreted this to imply a tectonic setting of metamorphism comparable to some modern orogenic belts, and that the southern granite-greenstone terrane possibly reflects lower crust exhumed during the 3.23 Ga tectonomagmatic event.

GEOLOGY OF THE STUDY AREA

The Schapenburg schist belt (Fig. 2) is one of many greenstone remnants included within and between the predominantly gneissic trondhjemite plutons to the south of the Barberton greenstone belt (Fig. 1). Lithologically, the xenoliths have been correlated with the lowermost formations of the Onverwacht Group (e.g., Viljoen and Viljoen, 1969; Anhaeusser, 1980; Anhaeusser and Robb, 1980). They predominantly consist of mafic and ultramafic schists, interlayered banded iron formation and chert, locally developed felsic agglomerates and tuffs, as well as a minor clastic metasedimentary unit that was deposited between *c.* 3530 and 3431 Ma (Dziggel et al., 2001).

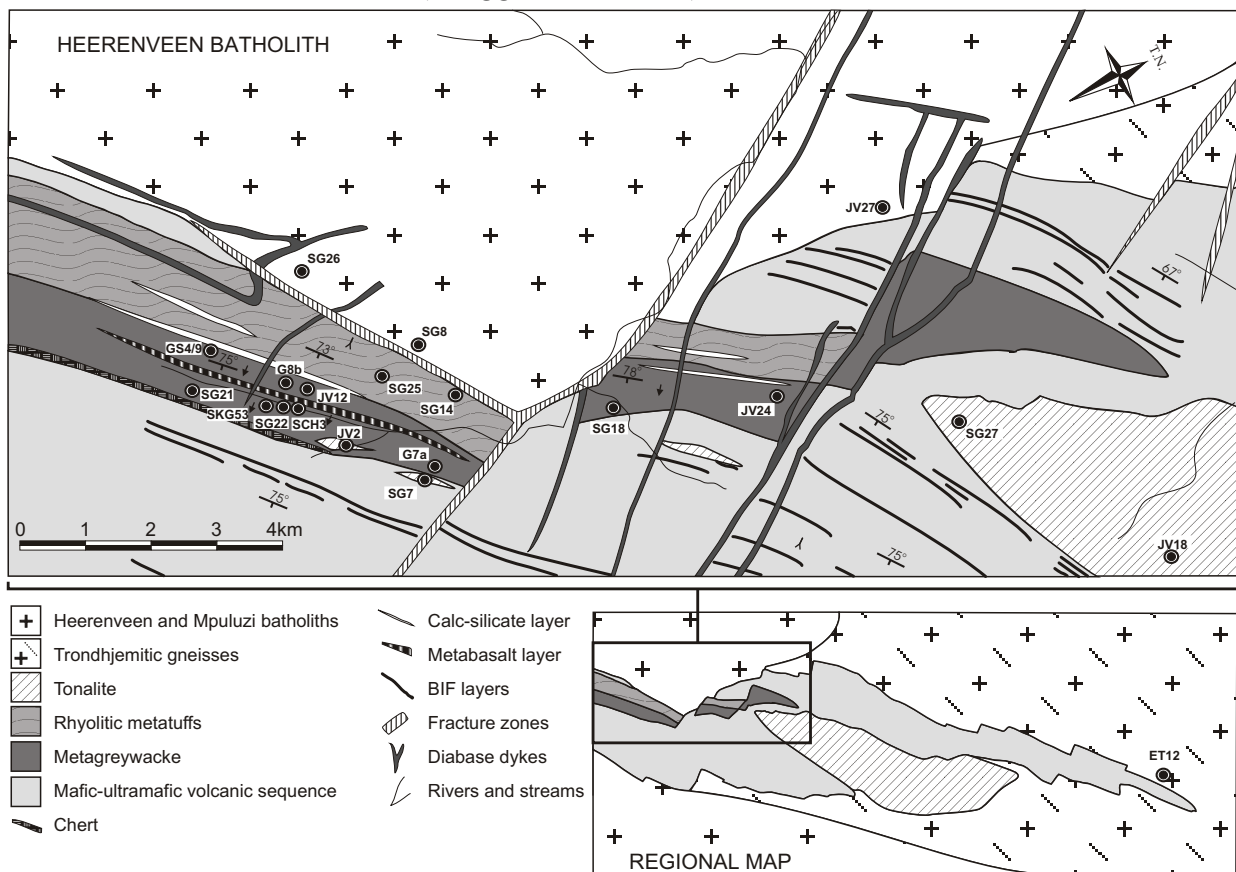


Figure 2: The geology of the Schapenburg schist belt, modified after Anhaeusser (1983). Only dykes and fracture zones that developed along faults that displace the metasedimentary rocks have been included. Inset map shows area enlarged.

The strong bedding-parallel foliation in most greenstone remnants is subvertical, and can usually be traced into the gneissic fabric of the adjacent trondhjemites. Despite this, trondhjemites that crosscut the original layering in several greenstone remnants, as well as the numerous greenstone xenoliths within them, indicate a primary intrusive relationship (Robb, 1983).

The Schapenburg schist belt was first described by Anhaeusser (1983) and consists of a well-defined layered mafic-ultramafic volcanic sequence, as well as a substantial

metasedimentary package that Anhaeusser regarded as an uniquely preserved sedimentary sequence found within or adjacent to the predominantly ultramafic extrusive lower Onverwacht Group.

The stratigraphy of the Schapenburg schist belt has a predominant northeasterly trend and dips to the southeast with an average angle of 75° SE. The schist belt is flanked by migmatitic trondhjemitic gneisses to the northwest and southeast, although close to the western limit of the mapped outcrop area the belt is directly in contact with younger granodiorites of the Heerenveen batholith (Anhaeusser, 1983). The central portion of the belt is split into two limbs by the intrusion of a small tonalite pluton (Table 1). Small lensoid pods of tonalitic material also intrude the schist belt. Within the southeastern limb of the belt the mafic-ultramafic volcanic sequence is very well preserved in local low-strain domains and individual komatiitic lava flows have been mapped in detail (Anhaeusser, 1983, 1991), allowing for reliable identification of the younging direction to the southeast.

Table 1: Representative rock compositions from the Schapenburg schist belt and surrounding granitoids. Sample positions are marked on Figure 2. Sample numbers in italics are from Anhaeusser (1983)

	Metatuff		Metaturbidites							Trond.	Tonalite				Adamellite		
	SG14	SG25	SG7	SG18	SG21	SG22	JV12	JV24	ET12	JV2	JV18	SG17	SG27	SG26	SG8	JV27	
SiO ₂	73.1	75.6	54.8	57.7	49.7	59.2	50.8	59.0	73.8	69.9	66.0	69.5	68.6	73.0	75.5	72.8	
TiO ₂	0.2	0.2	0.2	0.3	0.4	0.2	0.3	0.7	0.3	0.4	0.5	0.2	0.2	0.2	0.2	0.3	
Al ₂ O ₃	12.6	11.6	10.6	14.0	8.6	12.0	8.2	14.5	13.7	16.2	16.0	15.7	15.5	13.9	14.5	13.5	
Fe ₂ O ₃	2.7	2.5	22.3	11.4	16.2	14.5	32.2	12.7	2.2	2.8	3.9	3.3	3.4	1.8	2.0	1.8	
MnO	0.1	0.1	0.4	0.2	0.3	0.2	0.8	0.2	0.0	0.0	0.1	0.0	0.0	0.0	0.0	0.1	
MgO	1.9	2.1	5.8	9.0	12.2	4.5	4.6	5.6	0.8	1.2	2.2	1.0	1.1	0.3	0.3	0.6	
CaO	1.1	1.8	1.8	1.3	11.0	1.4	2.0	1.5	2.9	3.3	4.3	2.7	3.1	0.9	0.7	1.0	
Na ₂ O	2.3	3.0	1.2	1.5	0.7	0.9	1.4	1.6	4.2	3.6	4.1	4.1	4.3	3.4	1.7	3.0	
K ₂ O	3.8	2.4	1.7	2.3	0.3	3.0	0.2	2.6	1.1	1.6	2.3	1.8	1.9	5.3	5.3	5.3	
P ₂ O ₅	0.1	0.1	0.1	0.1	0.1	0.1	0.1	0.1	0.1	0.1	0.2	0.1	0.1	0.1	0.1	0.1	
LOI	0.9	0.9	0.6	0.8	0.8	3.4	0.7	1.1	0.5	1.8	1.2	0.8	0.8	0.5	0.9	0.8	
Total	98.7	100.3	99.5	98.6	100.2	99.3	101.2	99.5	99.5	100.8	100.8	99.5	99.2	99.4	101.2	101.0	
Mg#	0.74	0.77	0.51	0.76	0.75	0.55	0.36	0.64	0.59	0.63	0.69	0.55	0.56	0.40	0.37	0.57	
A	0.57	0.57	0.23	0.28	0.17	0.30	0.20	0.34	0.78	0.75	0.63	0.75	0.73	0.81	0.81	0.74	

The metasediments are developed as two distinctly different rock types in a wedge-shaped zone towards the southwestern end of the schist belt (Fig. 2). The metasediments of the western unit consist of a 300m-thick sequence of finely banded quartz-feldspar-biotite schists of granitic composition (Table 1) that are interpreted to be rhyolitic metatuffs. Locally, within low strain domains, the 2 to 5 cm scale compositional banding of these rocks can be recognised as graded bedding. Also within these zones cross-bedding is preserved (Fig. 3a) providing evidence of a southeasterly younging direction that is consistent with that determined for the overlying komatiitic sequence. The metasediments of the eastern unit consist of a 200m-thick sequence of interbanded mica-garnet schists and magnetite-grunerite-quartz schists (Fig. 3b). The metapelitic mica-rich bands are typically 10cm thick and locally can be seen to grade into more quartz-rich metagreywacke compositions towards the eastern (top) side of individual layers. The metagreywacke layers are typically 4 to 5 cm thick. Collectively, these observations led Anhaeusser (1983) to the conclusion that these banded rocks represent a metamorphosed turbidite deposit. In places this unit contains abundant cordierite porphyroblasts. These are flattened and

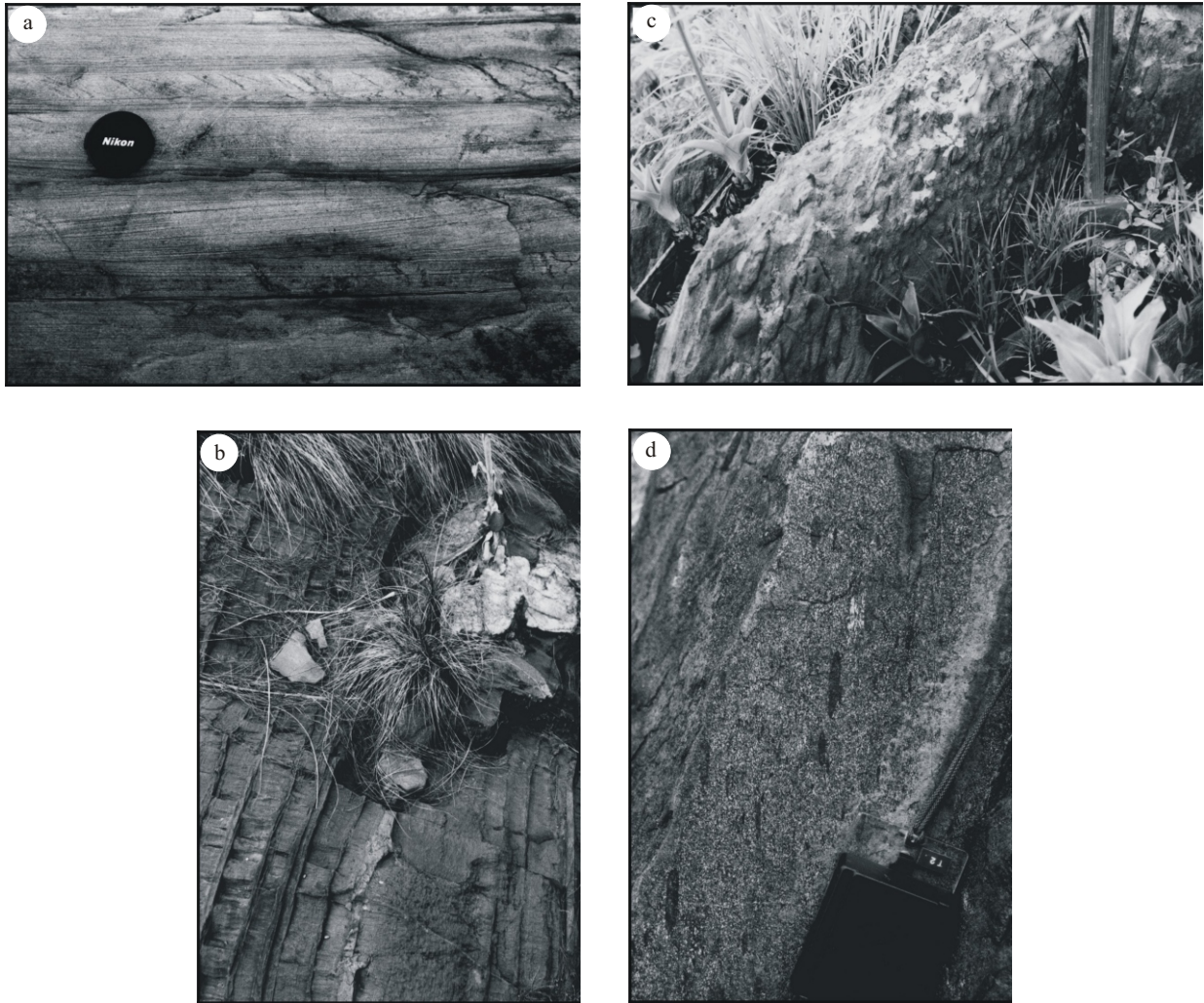


Figure 3: (a) Well preserved cross-bedding in a low strain domain within the metatuff unit. (b) Typical rhythmic banding of quartz-rich and mica-rich layers in the metaturbidite unit. The narrow layers that weather positively are 2 to 3 cm wide quartz-grunerite-magnetite schists. (c) Elongated cordierite porphyroblasts defining a strong down-dip lineation in the metaturbidite unit close to the contact with the overlying ultramafic volcanic unit. (d) Elongated mafic clasts in an intermediate composition agglomerate layer from within the metaturbidite sequence that define the same lineation orientation as the cordierite porphyroblasts.

elongated within the strongly developed layer-parallel foliation (averaging $43/76^{\circ}$ E), to form elliptical strain markers up to 10 cm in length (Fig. 3c) that define a well-developed down-dip lineation. A metavolcanic mafic rock layer developed within the metaturbidite sequence contains a 60 cm-wide agglomerate layer of intermediate composition. Mafic clasts within the agglomerate record the same later parallel flattening and down-dip extension recorded by the cordierite porphyroclasts (Fig. 3d). The metasedimentary sequence is separated from the overlying mafic-ultramafic volcanic sequence by a band of quartzite that Anhaeusser (1983) interpreted as a metamorphosed and recrystallised chert layer. Representative major element compositions for both metasedimentary units are listed in Table 1.

GEOCHRONOLOGY

The geochronology of the Schapenburg schist belt has formed the focus of a major study that has analysed zircon grains from the sediments, from various felsic igneous rocks associated with the belt, and monazites from a pegmatite within the belt (Armstrong et al., in prep). Only results specifically relevant to the timing of the metamorphism are discussed here. Zircons extracted from both the metatuff (sample SG25) and the tonalite pluton in the middle of the belt (sample SG27) were subjected to U-Th-Pb SHRIMP analyses performed at the Research School for Earth Sciences (RSES) at the Australian National University, Canberra. Zircons were handpicked, mounted in epoxy resin and polished. SEM cathodoluminescence imagery was used to determine the internal structures of the zircons prior to analysis. The zircon population extracted from the tonalite consisted of euhedral clear crystals of magmatic origin. The weighted $^{207}\text{Pb}/^{206}\text{Pb}$ mean of a group of 10 highly concordant zircons define an age of 3231 ± 5 Ma. This is, within error, similar to the age of the Kaap Valley pluton, which is also tonalitic in composition. The zircon population extracted from the metatuff is dominated by detrital grains, the youngest of which have an age of 3240 ± 4 Ma, defining the maximum age for the lower portions of the metasedimentary sequence exposed at Schapenburg, and thus also the maximum age of the metamorphism. The minimum age of the metamorphism is defined by the age of the tonalite that intrudes the metasediments.

METAMORPHISM OF THE METATURBIDITE SEQUENCE

The aluminous nature of the original shale components in the metaturbidite sequence has produced a range of useful metamorphic assemblages for which mineral chemical data have been obtained (Table 2, Fig. 2). The assemblages recorded include: (1) Grt + Crd + Ged + Bt + Qtz (SKG53); (2) Grt + Crd + Ged + Cumm + Bt + Pl + Qtz (G8b); (3) Grt + Cumm + Bt + Qtz (G7a); (4) Crd + Anth + Cumm + Bt + Chl + Qtz (GS4/9); and (5) Crd + Bt + Qtz (SCH3). Other assemblages recognised are Crd + Bt + Sill + Qtz and Crd + Bt + Mus + And + Qtz.

The Schapenburg metasediments are typified by schistose textures and a high degree of textural equilibration. There is no textural evidence for prograde reactions, no relic prograde phases occur as inclusions in the cordierite or garnet porphyroblasts (Fig. 4), and the only reaction textures evident are the product of rare retrogression. Chlorite has formed by replacement of biotite and cordierite, and an andalusite + muscovite assemblage has formed by retrogression of cordierite, biotite and sillimanite. These retrograde phenomena appear to correlate with proximity of the samples to the contact between the metasediments and the Heerenveen batholith.

The foliation in the metasediments is defined by the alignment of biotite crystals and the flattening and elongation of poikiloblastic cordierite porphyroblasts. Within the cordierite porphyroblasts aligned magnetite inclusion arrays define an earlier foliation at a moderate angle to the pervasive bedding-parallel foliation that now dominates the schist belt (Fig. 4). Garnet and orthoamphibole porphyroblasts overgrow this foliation (Fig. 4). Collectively, this evidence suggests that cordierite was a component of the prograde assemblage; that the deformation responsible for rodding of the cordierite porphyroclasts and agglomerate clasts occurred in the cordierite stability field during prograde metamorphism; and, that the metamorphic peak was attained once penetrative deformation had ceased.

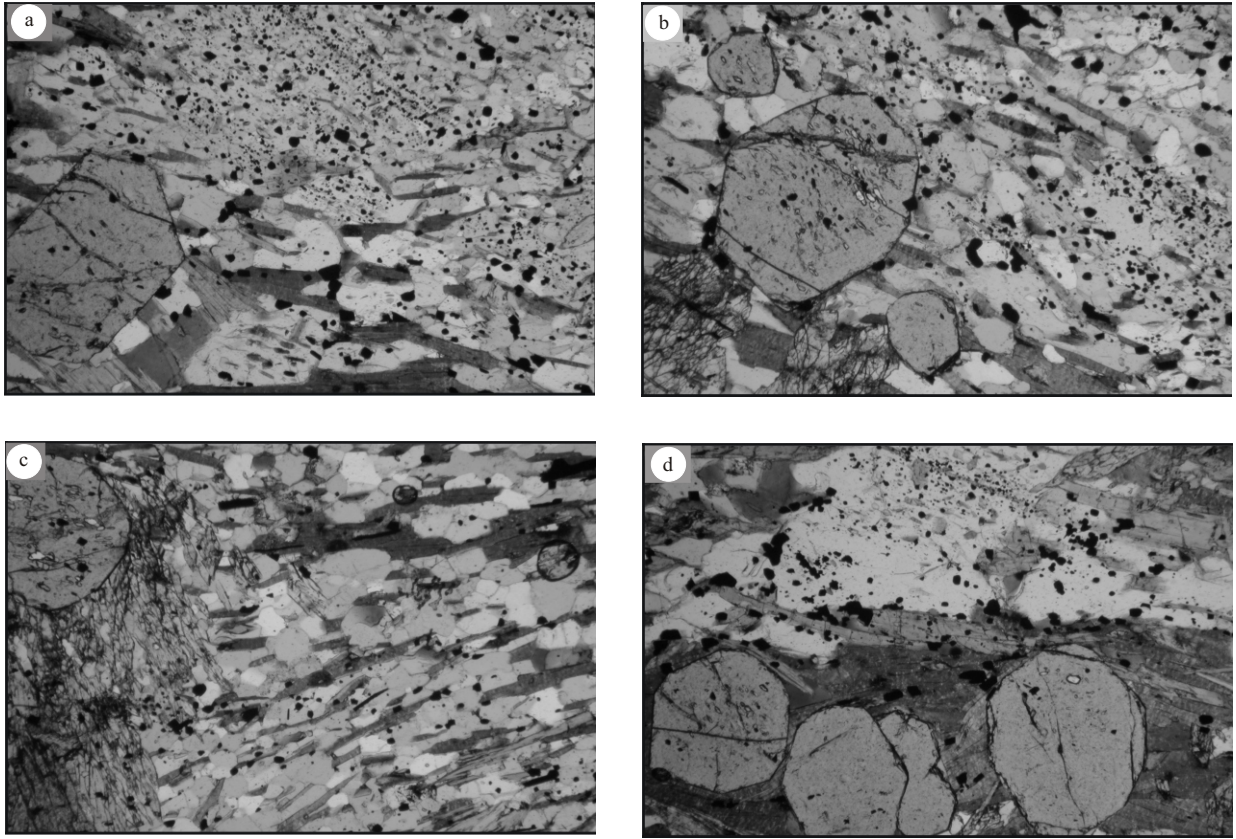


Figure 4: Typical mineral textures developed in the aluminous bands of the metaturbidite sequence in the Schapenburg schist belt. The poikiloblastic cordierite porphyroblasts commonly contain linear arrays of magnetite inclusions at an angle to the dominant layer parallel foliation (a and d). Garnet and orthoamphibole have commonly grown across this foliation (b, c and d). Poikiloblastic garnet porphyroblasts occasionally contain sigmoidal inclusion trails of quartz and magnetite indicating the presence of garnet during deformation (c), despite the clear evidence for the post-deformational nature of the dominant phase of garnet growth.

MINERAL CHEMISTRY

Individual mineral compositions within each rock are very uniform as can be seen from the representative mineral compositions for the samples studied (Table 2). Table 3 lists averaged mineral end-member activities, as well as the number of grains analysed and the standard deviation. Garnet from these rocks shows an almost completely flat compositional profile, with only slight zoning of the outermost 50 μm of the crystals to higher Mn and Fe^{2+} , and lower Mg. This is interpreted as testifying to slight retrograde re-equilibration of the peak assemblage.

PEAK METAMORPHIC CONDITIONS

Six established garnet-biotite geothermometers have been applied to samples SKG53, G8b and G7a, at a nominal pressure of 5 kbar (Table 4). The activities used are listed in Table 3 and represent values derived from averaged biotite compositions and the average composition of the interior of garnet crystals. These compositions are considered

Table 2: Representative mineral compositions from the Schapenburg metasediments SKG 53, G8b, G7a, GS4/9 and SCH3

	SKG 53					G8b					G7a					GS4/9					SCH3		
	Wt%	Grt	Crđ	Ged	Bt	Grt	Crđ	Ged	Cumm	Bt	Pl	Grt	Cumm	Bt	Crđ	Anth	Cumm	Bt	Chl	Crđ	Bt		
SiO ₂		37.61	48.66	44.47	36.56	37.63	48.80	42.34	52.92	36.68	60.94	37.72	52.75	36.00	48.59	53.69	54.16	37.68	26.22	47.68	34.66		
TiO ₂		0.09	0.01	0.05	1.63	0.04	0.03	0.38	0.01	1.63	0.04	0.08	0.00	1.72	0.00	0.07	0.07	1.50	0.01	0.00	2.58		
Al ₂ O ₃		20.82	33.02	12.76	17.01	20.87	33.00	15.16	1.50	17.45	25.09	21.07	1.60	17.04	32.89	2.37	1.38	16.69	21.89	32.20	19.67		
Cr ₂ O ₃		0.17	0.01	0.11	0.18	0.02	0.03	0.11	0.12	0.07	0.00	0.04	0.03	0.06	0.00	0.08	0.08	0.97	0.65	0.00	0.09		
Fe ₂ O ₃		0.67	0.00	0.00	0.00	0.00	0.00	0.00	0.00	0.00	0.00	0.47	0.00	0.00	0.00	0.00	0.00	0.00	0.00	0.00	0.00		
FeO		31.62	6.81	25.72	18.01	32.23	6.55	25.18	25.41	17.96	0.27	32.88	26.13	19.45	5.31	21.51	21.87	13.39	16.16	10.84	21.95		
MnO		3.75	0.16	0.64	0.00	3.45	0.06	0.60	0.41	0.00	0.00	2.60	0.21	0.00	0.00	0.07	0.14	0.00	0.00	0.23	0.00		
MgO		4.21	9.09	12.16	12.56	4.09	9.15	11.15	15.99	12.52	0.00	4.07	15.58	11.66	10.37	19.07	19.03	14.96	20.86	6.25	7.27		
CaO		1.76	0.00	0.31	0.06	1.58	0.00	0.35	0.23	0.02	6.48	1.92	0.35	0.08	0.00	0.20	0.27	0.00	0.03	0.01	0.13		
Na ₂ O		0.00	0.73	1.57	0.60	0.00	0.84	2.02	0.49	0.45	8.05	0.00	0.72	0.47	0.48	0.57	0.40	0.49	0.00	0.70	0.53		
K ₂ O		0.00	0.04	0.03	8.84	0.00	0.05	0.02	0.00	9.18	0.00	0.00	0.05	8.84	0.00	0.00	0.00	8.77	0.00	0.05	8.85		
Total		100.69	98.54	97.82	95.45	100.57	98.51	97.30	97.08	95.94	100.87	100.86	97.42	95.32	97.64	97.62	97.39	94.46	85.74	97.96	95.72		
Formula		vi = 5	18(O)	23(O)	11(O)	vi = 5	18(O)	23(O)	23(O)	11(O)	8(O)	vi = 5	23(O)	11(O)	18(O)	23(O)	23(O)	11(O)	14(O)	18(O)	11(O)		
Si		2.99	4.98	6.65	2.76	3.00	4.99	6.38	7.86	2.75	2.69	2.99	7.84	2.74	4.98	7.77	7.86	2.80	2.69	5.00	2.66		
Ti		0.01	0.00	0.01	0.09	0.00	0.00	0.04	0.00	0.09	0.00	0.01	0.00	0.10	0.00	0.01	0.01	0.08	0.00	0.00	0.15		
Al		1.95	3.98	2.25	1.51	1.96	3.98	2.69	0.26	1.54	1.31	1.97	0.28	1.53	3.97	0.41	0.24	1.46	2.65	3.98	1.78		
Cr		0.01	0.00	0.01	0.01	0.00	0.00	0.01	0.01	0.00	0.00	0.00	0.00	0.00	0.00	0.01	0.01	0.06	0.05	0.00	0.01		
Fe ³⁺		0.04	0.00	0.00	0.00	0.04	0.00	0.00	0.00	0.00	0.00	0.03	0.00	0.00	0.00	0.00	0.00	0.00	0.00	0.00	0.00		
Fe ²⁺		2.10	0.58	3.22	1.11	2.15	0.56	3.17	3.16	1.13	0.01	2.18	3.25	1.24	0.46	2.60	2.66	0.83	1.39	0.95	1.41		
Mn		0.25	0.01	0.08	0.00	0.23	0.01	0.08	0.05	0.00	0.00	0.18	0.03	0.00	0.00	0.01	0.02	0.00	0.00	0.02	0.00		
Mg		0.50	1.39	2.71	1.41	0.49	1.39	2.50	3.54	1.40	0.00	0.48	3.45	1.32	1.58	4.11	4.12	1.66	3.19	0.98	0.83		
Ca		0.15	0.00	0.05	0.01	0.14	0.00	0.06	0.04	0.00	0.31	0.16	0.06	0.01	0.00	0.03	0.04	0.00	0.00	0.00	0.01		
Na		0.00	0.14	0.46	0.09	0.00	0.17	0.59	0.14	0.07	0.69	0.00	0.21	0.07	0.10	0.16	0.11	0.07	0.00	0.14	0.08		
K		0.00	0.01	0.01	0.85	0.00	0.01	0.00	0.00	0.88	0.00	0.00	0.01	0.86	0.00	0.00	0.00	0.83	0.00	0.01	0.87		
Total		7.99	11.10	15.44	7.84	8.00	11.11	15.53	15.07	7.86	5.00	8.00	15.13	7.86	11.08	15.10	15.06	7.80	9.96	11.08	7.78		

Table 3: Average calculated mineral end-member activities for a condition of T=650°C. The activity models used are listed in brackets after each mineral name

Garnet (Berman, 1990)				Cordierite (ideal ionic)				Gedrite (ideal ionic)			
Sample End M.				Sample End M.				Sample End M.			
SKG53	Alm	0.33	0.0120	SKG53	Mg-Crd	0.50	0.01	SKG53	Anth	0.00012	0.00004
(n = 29)	Py	0.0066	0.0008	(n = 30)	Fe-Crd	0.087	0.004	(n = 18)	Ged	0.0015	0.0002
	Grs	0.00027	0.00006						Mg#	0.459	0.007
	Mg#	0.188	0.007								
G8b	Alm	0.34	0.014	G8b	Mg-Crd	0.50	0.01	GS4/9	Anth	0.016	0.002
(n = 31)	Py	0.0064	0.0010	(n = 16)	Fe-Crd	0.087	0.003	(n = 17)	Ged	0.0000360	0.00003
	Grs	0.00022	0.000036	SCH3	Mg-Crd	0.28	0.01		Mg#	0.61	0.003
	Mg#	0.186	0.010	(n = 7)	Fe-Crd	0.22	0.01				
G7a	Alm	0.36	0.01	GS4/9	Mg-Crd	0.61	0.006	G8b	Anth	0.0000510	0.000029
(n = 34)	Py	0.0068	0.0006	(n = 14)	Fe-Crd	0.049	0.002	(n = 27)	Ged	0.0017	0.0002
	Grs	0.00041	0.00005						Mg#	0.44	0.002
	Mg#	0.184	0.005								
Cummingtonite (ideal ionic)				Plagioclase (Elkins and Grove, 1990)				Biotite (Holland and Powell, 1998)			
Sample End M.				Sample End M.				Sample End M.			
G7a	Cumm	0.0056	0.0003	G8b	Ab	0.66	0.003	SKG53	Phl	0.075	0.005
(n = 6)	Grun	0.0036	0.0004	(n = 12)	An	0.42	0.003	(n = 25)	Ann	0.041	0.003
	Mg#	0.516	0.004						East	0.047	0.002
									Mg#	0.551	0.008
								G8a	Phl	0.082	0.004
								(n = 22)	Ann	0.042	0.003
									East	0.048	0.003
									Mg#	0.555	0.008
								G7a	Phl	0.068	0.003
								(n = 24)	Ann	0.052	0.004
									East	0.038	0.003
									Mg#	0.523	0.010
								SCH3	Phl	0.0185	0.002
								(n = 10)	Ann	0.072	0.005
									East	0.031	0.002
									Mg#	0.389	0.010
								GS4/9	Phl	0.130	0.005
									Ann	0.019	0.002
									East	0.046	0.003
									Mg#	0.655	0.011

representative of peak of metamorphic equilibration. The narrow, slightly more Fe-rich garnet rims produced lower temperatures. At 5 kbar, the calculated temperatures average at 606°C, 601°C and 629°C for samples SKGS3, G8b and G7a, respectively. Because Fe-Mg-exchange equilibria have large dP/dT ($>130\text{bar}/^\circ\text{C}$), the calculated temperatures are relatively insensitive to pressure. The samples are derived from a small enough area (Fig. 2) such that the peak metamorphic conditions could not have varied significantly between samples. Thus, a peak-metamorphic temperature estimate of $620 \pm 50^\circ\text{C}$ is probably a reasonable estimate based on garnet-biotite thermometry alone.

Three calibrations of the garnet-cordierite thermometer have been applied to samples SKG53 and G8b (Table 4) at the same pressure used for garnet-biotite thermometry. This thermometry provides identical averaged temperatures for both samples of 625°C at 5 kbar,

Table 4: Calculated Fe-Mg exchange thermometry temperatures at 5 kbar for the Schapenburg metasediments. The following calibrations of the garnet-biotite thermometer are represented: T = Thompson (1976); H&L = Holdaway and Lee (1977); F&S = Ferry and Spear (1978); P&L = Perchuk and Lavrenteva (1983); H&S = Hodges and Spear (1982); and B = Battacharya et al. (1992). The results of the Thompson (1976) (T), Holdaway and Lee (1977) (H&L) and Battacharya et al. (1988) (B') calibrations of the garnet-cordierite thermometer are also listed

	Garnet - Biotite						Garnet - Cordierite		
	T	H&L	F&S	P&L	H&S	B	T	H&L	B'
StockGS3	616	598	604	606	605	606	597	589	689
G8b	611	593	597	603	598	604	596	588	689
G7a	639	617	634	623	636	626			

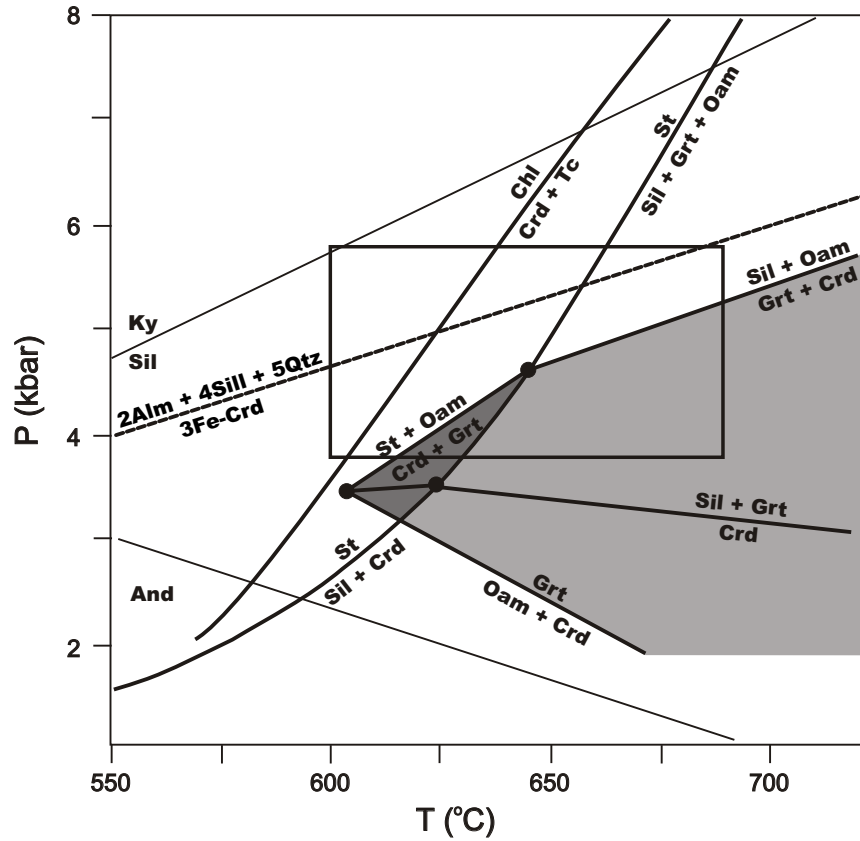


Figure 5: The petrogenetic grid of Hudson and Harte (1985) for K_2O -poor metapelites with the thermobarometry data from the Schapenburg metasediments superimposed as the central box. The box includes the position of the calculated pressure-temperature estimates, as well as the calculated errors. The possible assemblages documented in this study equilibrated at conditions above those of the reaction $Oam + Crd = Grt$, and below those of the reactions $Crd + Grt = St + Oam$ and $Grt + Crd = Sil + Oam$. Thus the grid constrains these assemblages to the entire shaded area. A previous study (Anhaeusser, 1983) reported the presence of staurolite. This would further constrain the pressure-temperature range for peak metamorphism to the darkly shaded area. Staurolite was not identified in this study.

although calculations carried out using the thermodynamic data of Holland and Powell (1998) with version 2.75 (1998) of the THERMOCALC program (Powell and Holland, 1988) in the 'average PT calculation' mode and assuming fluid-present conditions and $a_{\text{H}_2\text{O}} = 1$, produced peak-metamorphic conditions of $654 \pm 79^\circ\text{C}$ and 5.4 ± 1.2 kbar (fit index = 0.70) for sample SKG53, and $633 \pm 74^\circ\text{C}$ and 4.8 ± 1.1 kbar (fit index = 0.83) for sample G8b. The petrogenetic grid of Hudson and Harte (1985) for K_2O -poor metapelites indicates a broad field of garnet + cordierite + orthoamphibole coexistence at moderate to low pressures and at temperatures above 600°C (Fig. 5) which overlaps only the lower part of the calculated pressure range. This is corroborated by the absence of sillimanite in the garnet-cordierite-quartz-bearing samples which are constrained to have crystallised on the low-P side of the P-sensitive equilibrium $3 \text{ Fe-Crd} = 2 \text{ Alm} + 4 \text{ Sil} + 5 \text{ Qtz}$; when calculated for sample SKG53, the curve for this equilibrium yields a maximum pressure of 5.3 ± 0.5 kbar at 650°C (Fig. 5). In general, however, the thermobarometric data agree with one another, within error, and indicate peak-metamorphic conditions of $640 \pm 40^\circ\text{C}$ and 4.8 ± 1.0 kbar.

DISCUSSION

The age of the detrital zircons in the metasediments indicates that these are equivalents of Fig Tree Group rocks formed some 200 Ma after the komatiitic Onverwacht Group sequence that structurally overlies them. In the Schapenburg schist belt these metasediments have been metamorphosed to amphibolite facies conditions of 4.8 ± 1 kbar (depth = 17 ± 3 km) and $640 \pm 40^\circ\text{C}$ that imply a geothermal gradient of $38 \pm 13 / -9^\circ\text{C km}^{-1}$. The timing of prograde metamorphism is constrained by the age of a syntectonic tonalite intrusion at 3231 ± 5 Ma, linking this metamorphism firmly with the *c.* 3230 Ma terrane accretion event in the Barberton greenstone belt. The peak metamorphic conditions at Schapenburg post-dated the deformation that produced the crustal thickening recorded by both the metamorphism and stratigraphy of the schist belt. This has produced an annealing of the principal structural break between the Onverwacht and Fig Tree Groups, which is now marked by a quartzitic layer with an equigranular texture, originally interpreted to be a metamorphosed chert. In view of the findings of this study the position of this layer indicates that it is more likely to be an annealed quartz-rich fault rock. The elongation of original agglomerate clasts and of cordierite porphyroblasts defines a strong down-dip lineation that is consistent with tectonic transport of the Onverwacht sequence over the metasediments during prograde metamorphism. This evidence for crustal thickening by a thrust-stacking process, peak PT conditions consistent with metamorphism in response to the establishment of a high geothermal gradient of *c.* 40°C km^{-1} , and the abundant evidence for synmetamorphic calc-alkaline magmatism, create clear links with modern convergent margin processes. The Fig Tree rocks are regarded as the sedimentary response to tectonic basin closure preceding the accretion of an allochthonous terrane onto the proto-Kaapvaal Craton. In the Schapenburg schist belt it is evident that the formation of these sediments and their burial to a depth of approximately 17 km occurred within a time-span of 10 Ma.

ACKNOWLEDGEMENTS

EGRI-HAL at the University of the Witwatersrand is gratefully thanked for support during GS's employment with the Institute, when most of this research was conducted. The National Research Foundation is thanked for research funding via grants to GS. Thanks are also due to the University of Manchester and RSES at ANU for access to analytical facilities by GTRD and RA respectively.

REFERENCES

- Anhaeusser, C. R. (1969). The stratigraphy, structure and gold mineralization of the Jamestown and Sheba Hills area of the Barberton Mountain Land. Ph.D thesis (unpubl.), Univ. Witwatersrand, Johannesburg, 322 pp.
- Anhaeusser, C. R. (1978). The geological evolution of the primitive earth evidence from the Barberton Mountain Land, 71-106. In: Tarling, D. H. (Ed.), *Evolution of the Earth's Crust*, Academic Press, London, 443 pp.
- Anhaeusser, C. R. (1980). A geological investigation of the Archaean granite-greenstone terrane south of the Boesmanskop syenite pluton, Barberton Mountain Land. *Trans. Geol. Soc. S. Afr.*, **83**, (1), 93-106.
- Anhaeusser, C. R. (1983). The geology of the Schapenburg greenstone remnant and surrounding Archaean granitic terrane south of Badplaas, Eastern Transvaal. *Spec. Publ. Geol. Soc. S. Afr.*, **9**, 31-44.
- Anhaeusser, C. R. (1986). Archaean gold mineralisation in the Barberton Mountain Land, 113-154. In: Anhaeusser, C. R., Maske, S. (Eds.), *Mineral Deposits of Southern Africa*, 1. *Geol. Soc. S. Afr.*, Johannesburg, 1020 pp.
- Anhaeusser, C. R. (1991). Schapenburg greenstone remnant, 107-115. In: Ashwal, L.D. (Ed.), *Two Cratons and an Orogen. Excursion Guidebook and Review Articles for a Field Workshop through Selected Archaean Terranes of Swaziland, South Africa and Zimbabwe*, IGCP Project 280, Dept. Geology, Univ. Witwatersrand, Johannesburg, 312 pp.
- Anhaeusser, C. R., Robb, L. J. (1980). Regional and detailed field and geochemical studies of Archaean trondhjemite gneisses, migmatites and greenstone xenoliths in the southern part of the Barberton Mountain Land, South Africa. *Precambrian Res.*, **11**, 373-397.
- Anhaeusser, C. R., Robb, L. J. (1981). Magmatic cycles and the evolution of the Archaean granitic crust in the Eastern Transvaal and Swaziland. *Spec. Publ. Geol. Soc. Aust.*, **7**, 457-467.
- Anhaeusser, C. R., Robb, L. J. (1983). Geological and geochemical characteristics of the Heerenveen and Mpuluzi batholiths south of the Barberton greenstone belt and preliminary thoughts on their petrogenesis. *Spec. Publ. Geol. Soc. S. Afr.*, **9**, 131-151.
- Anhaeusser, C. R., Viljoen, M.J. (1965). The base of the Swaziland System in the Barberton-Noordkaap- Louw's Creek area, Barberton Mountain Land. *Inform. Circ. Econ. Geol. Res. Unit, Univ. Witwatersrand, Johannesburg*, **25**, 32pp.

Anhaeusser, C. R., Robb, L. J., Barton, J. M. Jr., (1983). Mineralogy, petrology and origin of the Boesmanskop syeno-granite complex, Barberton Mountain Land, South Africa. *Spec. Publ. Geol. Soc. S. Afr.*, **9**, 169-183.

Armstrong, R. A., Compston, W., de Wit, M. J., Williams, I. S. (1990). The stratigraphy of the 3.5-3.2 Ga Barberton greenstone belt revisited; a single zircon ion microprobe study. *Earth Planet. Sci. Lett.*, **101**, 90-106.

Berman, R.G. (1990). Mixing properties of Ca-Mg-Fe-Mn garnets. *Amer. Mineral.*, **75**, 328-344.

Bhattacharya, A., Mazumdar, A.C., Sen, S.K. (1988). Fe-Mg mixing in cordierite: constraints from natural data and implications for cordierite-garnet geothermometry in granulites. *Amer. Mineral.*, **73**, 338-344.

Bhattacharya, A., Mohanty, L., Maji, A., Sen, S.K., Raith, M. (1992). Non-ideal mixing in the phlogopite-annite binary: constraints from experimental data on Mg-Fe partitioning and a reformulation of the biotite-garnet geothermometer. *Contrib. Mineral. Petrol.*, **111**, 87-93.

Brandl, G., de Wit, M. J. (1997). The Kaapvaal Craton, South Africa, 581-607. In: de Wit, M. J., Ashwal, L.D. (Eds.), *Greenstone Belts*. Oxford Monographs on Geology and Geophysics, **35**, 809 pp.

Brévar, O., Dupré, B., Allegre, C.J. (1986). Lead-lead age of komatiitic lavas and limitations on the structure and evolution of the Precambrian mantle. *Earth Planet. Sci. Lett.*, **77**, 293-302.

Cloete, M. (1991). An overview of metamorphism in the Barberton greenstone belt, 84-98. In: Ashwal, L.D. (Ed.), *Two Cratons and an Orogen. Excursion Guidebook and Review Articles for a Field Workshop through Selected Archaean Terranes of Swaziland, South Africa and Zimbabwe*, IGCP Project 280, Dept. Geology, Univ. Witwatersrand, Johannesburg, 312 pp.

Cloete, M. (1999). Aspects of volcanism and metamorphism of the Onverwacht Group lavas in the south-western portion of the Barberton greenstone belt. *Mem. Geol. Surv. S. Afr.*, **84**, 232 pp.

de Wit, M. J. (1982). Gliding and overthrust nappe tectonics in the Barberton greenstone belt. *J. Struct. Geol.*, **4**, 117-136.

de Wit, M. J. (1991). Archaean greenstone belt tectonism and basin development: some insights from the Barberton and Pietersburg greenstone belts, Kaapvaal Craton, South Africa. *J. Afr. Earth Sci.*, **13** (1), 45-63.

de Wit, M. J., Hart, R., Martin, A., Abbott, P. (1982). Archean abiogenic and probable biogenic structures associated with mineralized hydrothermal vent systems and regional metasomatism, with implications for greenstone belt studies. *Econ. Geol.*, **77** (8), 1783-1802.

de Wit, M. J., Hart, R. A., Hart, R. J. (1987). The Jamestown Ophiolite Complex, Barberton Mountain Land: a section through 3.5 Ga oceanic crust. *J. Afr. Earth Sci.*, **6**, 681-730.

de Ronde, C.E.J., de Wit, M.J. (1994). The tectonothermal evolution of the Barberton greenstone belt, South Africa: 490 million years of crustal evolution. *Tectonics*, **13**, 983-1005.

de Ronde, C.E.J., Kamo, S.L. (2000). An Archaean arc-arc collisional event: a short-lived (*ca* 3 *Myr*) episode, Weltevreden area, Barberton greenstone belt, South Africa. *J. Afr. Earth Sci.*, **30** (2), 219-248.

de Wit, M.J., Hart, R.A., Hart, R.J. (1987). The Jamestown Ophiolite Complex, Barberton Mountain Land: a section through 3.5 Ga oceanic crust. *J. Afr. Earth Sci.*, **5**, 681-730.

Dymoke, P., Sandiford, M. (1992). Phase relationships in Buchan facies series pelitic assemblages: calculations with application to andalusite-staurolite parageneses in the Mount Lofty Ranges, South Australia. *Contrib. Mineral. Petrol.*, **110**, 121-132.

Dziggel, A., Stevens, G., Poujol, M., Anhaeusser, C. R., Armstrong, R. A. (2001). Metamorphism of the granite-greenstone terrane south of the Barberton greenstone belt, South Africa: an insight into the tectono-thermal evolution of the lower portions of the Onverwacht Group. *Inform. Circ. Econ. Geol. Res. Inst., Univ. Witwatersrand, Johannesburg*, **352**, 35 pp.

Elkins, L.T., Grove, T.L. (1990). Ternary feldspar experiments and thermodynamic models. *Amer. Mineral.*, **75**, 544-559.

Ferry, J. M., Spear, F. S. (1978). Experimental calibration of the partition of Fe and Mg between garnet and biotite. *Contrib. Mineral. Petrol.*, **66**, 113-117.

Hamilton, P.J., Evensen, M.N., O'Nions, R.K., Smith, H.S., Erlank, A.J. (1979). Sm-Nd dating of the Onverwacht Group volcanics. *Nature*, **279**, 298-300.

Hodges, K.V., Spear, F.S. (1982). Geothermometry, geobarometry and the Al_2SiO_5 triple-point at Mt. Moosilauke, New Hampshire. *Amer. Mineral.*, **67**, 1118-1134.

Hoffman, S.E., Wilson, M., Stakes, D.S. (1986). An inferred oxygen isotope profile of Archaean oceanic crust, Onverwacht Group, South Africa. *Nature*, **321**, 55-58.

Holdaway, M.J., Lee, S.M. (1977). Fe,Mg-cordierite stability in high-grade pelitic rocks based on experimental, theoretical and natural observations. *Contrib. Mineral. Petrol.*, **B**, 175-198.

Holland, T.J.B., Powell, R. (1998). An internally consistent thermodynamic data set for phases of petrological interest. *J. Metamorphic Geol.*, **16**, 309-344.

Hudson, N.F.C., Harte, B. (1985). K_2O -poor aluminous assemblages from the Buchan Dalradian, and the variety of orthoamphibole assemblages in aluminous bulk compositions in the amphibolite facies. *Amer. J. Sci.*, **285**, 224-266.

Jahn, B. M., Shih, C.Y. (1974). On the age of the Onverwacht Group, Swaziland Sequence, South Africa. *Geochim. Cosmochim. Acta*, **38**, 873-885.

Kamo, S.L., Davis, D.W. (1994). Reassessment of Archean crustal development in the Barberton Mountain Land, South Africa based on U-Pb dating. *Tectonics*, **13** (1), 167-192.

Kröner, A., Todt, W. (1988). Single zircon dating constraining the maximum age of the Barberton greenstone belt, southern Africa. *J. Geophys. Res.*, **93**, 15329-15337.

López Martínez, M., York, D., Hall, C. M., Hanes, J. A. (1984). Oldest reliable $^{40}\text{Ar}/^{39}\text{Ar}$ ages for terrestrial rocks; Barberton Mountain komatiites. *Nature* **307**, 352-354.

Lowe, D. R. (1999). Geologic evolution of the Barberton greenstone belt and vicinity, 287-312. In: Lowe, D. R. and Byerly, G. R. (Eds.), *Geologic Evolution of the Barberton Greenstone Belt, South Africa. Spec. Paper Geol. Soc. Amer.*, **329**, 319pp.

Perchuk, L.L., Lavrent'eva, I.V. (1983). Experimental investigation of exchange equilibria in the system cordierite-garnet-biotite, 199-239. In: Saxena, S. K. (Ed.), *Kinetics and Equilibrium in Mineral Reactions*, Springer-Verlag, New York, Vol. 3.

Powell, R., Holland, T.J.B. (1988). An internally consistent thermodynamic dataset with uncertainties and correlations: 3. Application methods, worked examples and a computer program. *J. Metamorphic Geol.*, **6**, 173-204.

Robb, L. J. (1983). The nature, origin and significance of Archaean migmatites in the Barberton Mountain Land: a new approach in the assessment of early crustal evolution. *Spec. Publ. Geol. Soc. S. Afr.*, **9**, 81-101.

Robb, L. J., Anhaeusser, C. R., van Nierop, D. A. (1983). The recognition of the Nelspruit batholith north of the Barberton greenstone belt and its significance in terms of Archaean crustal evolution. *Spec. Publ. Geol. Soc. S. Afr.*, **9**, 117-130.

Thompson, A. B. (1976). Mineral reactions in pelitic rocks: II. Calculation of some P-T-X (Fe,Mg) phase relations. *Amer.J. Sci.*, **276**, 425-454.

Viljoen, M. J., Viljoen, R. P. (1969). A proposed new classification of the granitic rocks of the Barberton region. *Spec. Publ. Geol. Soc. S. Afr.*, **2**, 153-180.

Ward, J.H.W. (1999). The metallogeny of the Barberton greenstone belt South Africa and Swaziland. *Mem. Geol. Surv. S. Afr.*, **86**, 108pp.

Wilkins, C. (1997). Regional and contact metamorphism, 5-29. In: de Wit, M. J., Ashwal, L. D. (Eds.), *Greenstone Belts. Oxford Monographs on Geology and Geophysics*, **35**, 809 pp.

Xie, X., Byerly, G. R., Ferrell, R. E., Jr. (1997). Ilb trioctahedral chlorite from the Barberton greenstone belt: crystal structure and rock composition constraints with implications to geothermometry. *Contrib. Mineral. Petrol.*, **126**, 275-291.